



Cite this: *Dalton Trans.*, 2016, **45**, 10989

Received 24th May 2016,
Accepted 9th June 2016

DOI: 10.1039/c6dt02087a

www.rsc.org/dalton

Versatile coordination of a reactive P,N-ligand toward boron, aluminum and gallium and interconversion reactivity†

M. Devillard,^a C. Alvarez Lamsfus,^b V. Vreeken,^a L. Maron^b and J. I. van der Vlugt*^a

The synthesis and reactivity of the first Group 13 complexes bearing a dearomatized phosphino-amido ligand **L** are reported, *i.e.* alane $\text{AlEt}_2(\text{L})$ **1**, gallane $\text{GaCl}_2(\text{L})$ **2** and borane $\text{B}(\text{Cl})(\text{Ph})(\text{L})$ **3**. The three complexes react very differently with Group 13 trihalogenides, providing access to zwitterionic *anti*-**3**· GaCl_3 and the unique bis(metalloid) **5**· BCl_2 , with the boron center part of a highly unusual anionic four-membered ring (charge on C) and Ga bound to P. The coordination chemistry and the various transformations are supported by DFT calculations, X-ray crystallography and multinuclear NMR spectroscopic data.

Introduction

The synthetic chemistry and reactivity of Group 13 complexes has recently attracted much attention, both with respect to the preparation of unsaturated derivatives¹ and for application in bond activation processes and homogeneous catalysis,² often in combination with a Lewis base as a “Frustrated Lewis Pair” (FLP).³ At the same time, the bioinspired strategy to combine proton-responsive (‘reactive’) ligands and (transition) metal centers has become prominent, resulting in novel coordination chemistry with applications in small molecule activation and metal–ligand bifunctional catalysis.⁴

One particular strategy that has come to the forefront in this context is the use of lutidine- and picoline-based P,N donor ligands that can undergo reversible dearomatization.⁵ Many transition metals coordinate strongly to both phosphorus and nitrogen in these ligands,⁶ and deprotonation of the ligand backbone merely generates a nucleophilic carbon center that does not engage in any direct interaction with the metal coordination sphere. No examples of transmetalation on complexes bearing lutidine- or picoline-derived P,N-ligands are known, to the best of our knowledge.⁷ The coordination chemistry of Group 13 metals and metalloids such as boron and aluminum is unexplored with this type of reactive ligand scaffold. Hence, the fundamental reac-

tivity of complexes bearing a dearomatized P,N ligand is currently unknown but it could be envisioned that other ligand coordination modes may be accessible with these elements.

To address both challenges, we decided to exploit the reversible dearomatization chemistry of P,N-ligands to generate the first examples of Group 13 species with a dearomatized pyridine ligand (see Scheme 1). This approach has allowed access to highly reactive aluminum, gallium and boron compounds stabilized by an anionic P,N-scaffold and to study their versatile reactivity with G13 trihalogenides.

Results and discussion

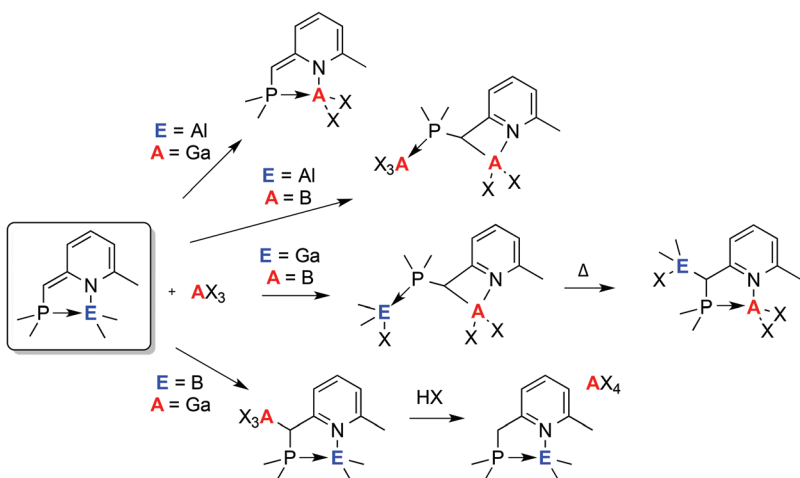
Reaction of the known bidentate P,N-ligand 2-(diphenylphosphinomethyl)-6-methyl-pyridine **L^H** with one molar equivalent of *n*-BuLi followed by electrophilic trapping with chlorodiethyl-aluminum (Scheme 2) resulted in the high yield synthesis of complex $\text{AlEt}_2(\text{L})$ **1** as a red oil, which was characterized by multinuclear NMR spectroscopy. Contrary to what was previously observed for the anion of lutidine,⁸ this reaction selectively generates an N-Group 13 element bond, with dearomatization of the N-heterocycle, rather than a C-Group 13 bond. The ¹H NMR spectrum contained three different resonances in the olefinic region (δ 5.28, 6.07 and 6.42) and a broad signal at δ 3.46 attributed to the methine proton of the $=\text{CH}-\text{PPh}_2$ arm. Only one resonance was observed for the two *tert*-butyl groups connected to phosphorus and both Et-groups at aluminum are also equivalent, confirming the *C_s* symmetry of the molecule. This compound features a clear P \rightarrow Al interaction, as evidenced by the broad ³¹P NMR signal at δ -0.9 ($\Delta\delta$ -36.2 relative to **L^H**) and the ²⁷Al NMR resonance at δ 162, which is characteristic of a four-coordinated amido-alane.⁹

^aHomogeneous, Bioinspired and Supramolecular, van 't Hoff Institute for Molecular Sciences, University of Amsterdam, Science Park 904, 1098 XH Amsterdam, The Netherlands. E-mail: j.i.vandervlugt@uva.nl

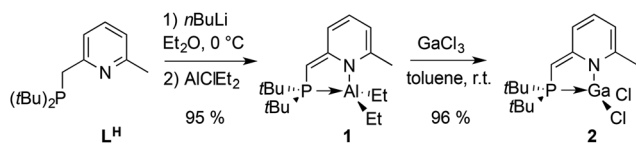
^bLaboratoire de Physique et Chimie des Nanoobjets, Université de Toulouse, INSA-UPS-CNRS (UMR 5215) 135, avenue de Rangueil, 31077 Toulouse cedex 4, France

† Electronic supplementary information (ESI) available. CCDC 1455266–1455269, 1481714. For ESI and crystallographic data in CIF or other electronic format see DOI: 10.1039/c6dt02087a





Scheme 1 Dearomatized Group 13 complexes of (phosphinomethyl)pyridine ligands described in this work, their reactivity with Group 13 trihalogenides and follow-up transformations.



Scheme 2 Preparation of the phosphorus-stabilized amidoalane **1** and subsequent transmetallation to form the parent gallane **2**.

Strikingly, the analogous reaction of **L^H** with AlCl_3 failed to generate any well-defined product.

To get insight into the geometric and electronic features of **1**, we optimized its structure using DFT calculations (Fig. 1).

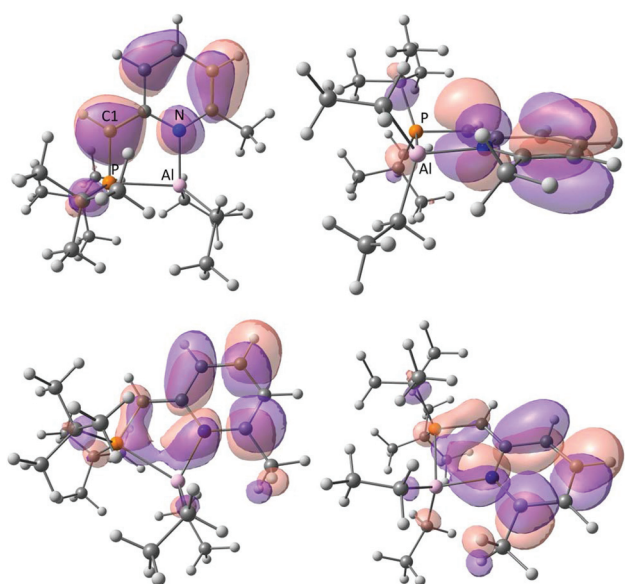


Fig. 1 (Top) HOMO and (bottom) LUMO frontier orbital plots (top and side views) for the phosphorus-stabilized amidoalane **1**.

The ligand framework adopts an almost planar configuration, with the phosphine and alane fragments slightly out of the N-heterocycle plane ($\angle \text{P2-C4-C6-C7}$ 177.8°, $\angle \text{Al1-N1-C6-C7}$ 174.6°). The N-heterocycle shows clear alternation of C-C and C=C bonds. The HOMO is mainly located on the C1 carbon (64.1%), suggesting that this alane complex with an anionic P,N ligand would likely react with electrophiles at the methine site, as previously established for *e.g.* MeOTf , CO_2 and nitrile electrophiles with either Cu and Ru complexes bearing dearomatized P,N pincers.¹⁰ However, common inorganic Lewis acids have not been employed as electrophiles, to the best of our knowledge.

We thus explored its reactivity toward gallium trichloride as a prototypical Lewis acid (Scheme 2). After addition of GaCl_3 to a solution of **1** in toluene at room temperature and work-up, the ^{31}P NMR spectrum contained only a very broad resonance at δ –3.1, while the ^1H NMR spectrum still showed the characteristic pattern for a dearomatized P,N backbone, but was lacking any signals for an AlEt_2 fragment. These spectroscopic data indicate a formal transmetallation from Al to Ga to generate $\text{GaCl}_2(\text{L})$ **2**, which was detected by HR-MS data (FD^+ , m/z = 390.04338), and AlClEt_2 . The structure of this gallane complex **2** was confirmed by X-ray structure determination on air-sensitive orange crystals of $\text{GaCl}_2(\text{L})$, obtained from a diethyl ether-toluene solution at r.t. (Fig. 2). In the crystal structure, the geometry around gallium is strongly pyramidal due to the interaction with the phosphine donor (sum of angles 331.9°). The N-heterocycle shows alternation of single and double C-C bonds, while the external C-C double bond lies in-between ($\text{C1-C2} = 1.394(2)$ Å) and the C1 carbon is clearly sp^2 hybridized.

The intriguing conversion of **1** into **2** may be envisioned to involve initial formation of a bis-metalloid intermediate **1-GaCl₃** with a C-Ga bond and a formally cationic Al-center, but this proposed intermediate could not be detected using **1**, despite various attempts. We hypothesized that such a bis-

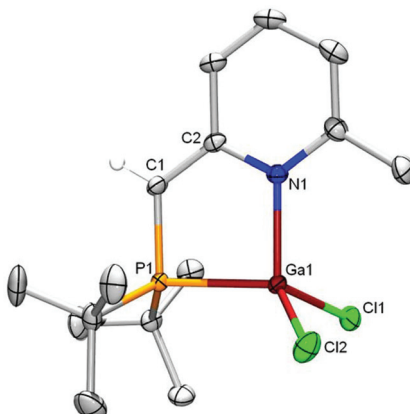


Fig. 2 Displacement ellipsoid plot (50% probability level) of 2. Hydrogen atoms (except for hydrogen on C1) are omitted for clarity. Selected bond lengths (Å) and angles (°): P1–Ga1 2.339(1); N1–Ga1 1.946(1); Ga1–Cl1 2.185(1); P1–C1 1.743(2); C1–C2 1.394(2); C2–C3 1.433(2); C3–C4 1.354(2); C4–C5 1.412(3); C5–C6 1.360(2); P1–Ga1–N1 90.0(1); P1–Ga1–Cl1 116.6(1); P1–C1–C2 120.8(1); P1–C1–C2–N1 1.3.

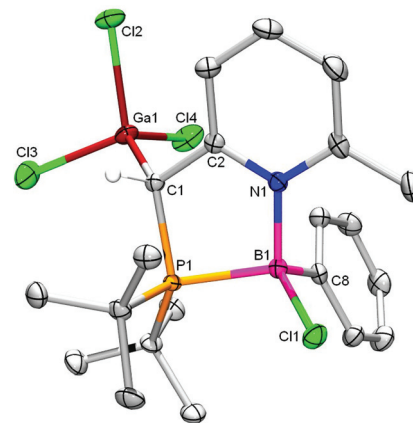


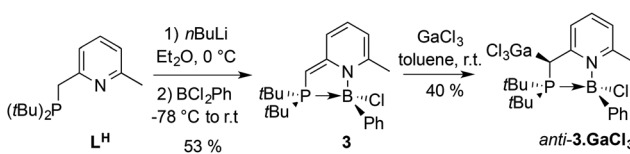
Fig. 3 Displacement ellipsoid plot (50% probability level) of *anti*-3-GaCl₃. Hydrogen atoms (apart from those on C1) are omitted for clarity. Selected bond lengths (Å) and angles (°): P1–C1 1.830(2); C1–C2 1.501(3); P1–B1 2.021(2); N1–B1 1.602(3); B1–Cl1 1.869(2); B1–C8 1.596(3); C1–Ga1 2.030(2); P1–B1–N1 98.0(1); P1–C1–Ga1 126.4(1); N1–B1–Cl1 111.3(1); N1–B1–C8 110.1(2); P1–C1–C2–N1 22.5.

metalloid structure could be more readily accessible with B instead of Al, as boron cations are known to be stable in tetra-coordinated environments (commonly termed boronium).¹¹ The boron analogue of **1** could be accessed *via* deprotonation of L^H and subsequent addition of Cl₂BPh (Scheme 3). Complex B(Cl)(Ph)(L) **3** was obtained in 53% yield as a very air-sensitive red oil that was completely characterized by multinuclear NMR and HR-MS (CSI [M + H]⁺, *m/z* 374.1976). The ³¹P NMR spectrum of **3** shows a broad resonance at δ 24.5 ($\Delta\delta$ = -10.8 ppm) and the doublet in ¹¹B NMR is found in the typical region for tetracoordinated boron atoms (δ 5.1, $^1J_{BP}$ = 106 Hz), confirming its connectivity to phosphorus. The ¹H NMR spectrum of **3** showed a doublet at δ 3.46 ($^2J_{HP}$ = 5.1 Hz) attributed to the proton of the =CH-PPh₂ arm.

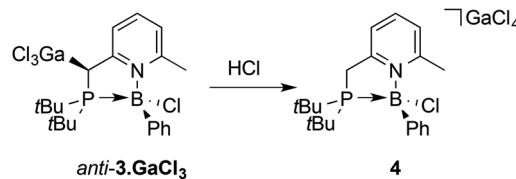
Addition of 1 eq. of GaCl₃ to **3** instantaneously yielded a yellow precipitate, which was characterized by a broad signal at δ 34.0 in the ³¹P NMR spectrum ($\Delta\delta$ = 9.5 ppm) and a slightly upfield shifted ¹¹B NMR signal (δ 5.6); ($\Delta\delta$ = 0.5 ppm). The presence of a doublet at δ 3.67 in the ¹H NMR spectrum with a relatively large $^2J_{HP}$ coupling constant of 13.4 Hz ($\Delta\delta$ = 8.3 Hz compared to **3**) indicates rearomatization of the N-heterocycle and supports addition of GaCl₃ to the methylene carbon spacer. Single crystal X-ray structure determination confirmed the diastereoselective formation of the formally

zwitterionic *anti*-3-GaCl₃ (*anti* refers to the relative positions of the chloride at boron and the GaCl₃ fragment with respect to the G13-pyridine plane, Fig. 3). The new C1–Ga1 bond is in the range of previously reported carbogallates.¹² The boronium fragment is strongly pyramidalized (sum of angles 333.5°). DFT calculations (Gaussian 09, B3PW91, 6-31G**) show that the *syn*-3-GaCl₃ diastereoisomer is 3.7 kcal mol⁻¹ higher in energy, which is within the upper limit of the precision of the methods. Heating a solution of *anti*-3-GaCl₃ for 10 h at 100 °C led to partial isomerization to *syn*-3-GaCl₃, as evidenced by multinuclear NMR spectroscopy.

Although there is some precedent for nucleophilic attack of dearomatized pincer transition metal complexes on a Group 13 Lewis acid,¹³ this reactivity is unprecedented for main group elements or metalloids. Moreover, given the propensity of GaCl₃ to act as halide scavenger toward main group halides, including boron for the generation of boron cations,¹⁴ the observed preference to act as electrophile in a carbon–gallium bond formation step is deemed highly remarkable. This bond is indeed reactive, as evidenced by the reaction of *anti*-3-GaCl₃ with HCl, which led to protonation at the methylene carbon with the formation of tetrachlorogallate salt **4** (Scheme 4), which was fully characterized, including by single crystal X-ray structure determination (Fig. 4).



Scheme 3 Preparation of the phosphorus-stabilized amidoborane **3** and its reaction with GaCl₃ to form the zwitterion *anti*-3-GaCl₃.



Scheme 4 Reaction of *anti*-3-GaCl₃ with HCl to give **4**.

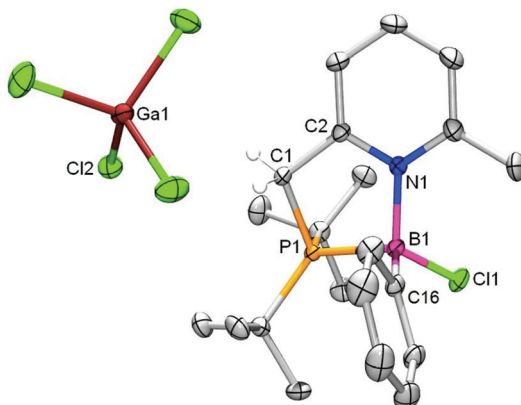


Fig. 4 Displacement ellipsoid plot (50% probability level) of **4**. Hydrogen atoms are omitted for clarity. Selected bond lengths (Å) and angles (°): P1–B1 2.018(2); N1–B1 1.608(2); B1–Cl1 1.859(2); B1–C16 1.597(3); P1–C1 1.817(2); C1–C2 1.502(2); P1–B1–N1 97.4(1); P1–B1–N1 109.3(1); P1–B1–C16 113.7(1); P1–C1–C2 105.4(1); P1–C1–C2–N1–27.3.

The electronegativity of Ga lies in-between that of B and Al. We decided to explore the reaction of gallane **2** with boron trichloride as Lewis acid in order to probe whether the resulting reactivity of these Group 13 elements bound to a dearomatized P,N ligand follows the same trend. Upon addition of BCl_3 to **2**, the bright orange reaction mixture turned colorless, which is diagnostic of re-aromatization (Scheme 5).

The broad ^{31}P NMR signal appeared at lower field (δ 31.1 ppm, $\Delta\delta$ –10.8 ppm) with no evidence for P–B coupling, indicative that the phosphine is still connected to gallium. In the ^1H NMR spectrum, the $=\text{CH}-\text{PPH}_2$ proton is deshielded (δ 3.93 ppm) and broadened due to scalar proximity of a ^{11}B nucleus (confirmed by $^1\text{H}\{^{11}\text{B}\}$ NMR analysis). Single crystal X-ray structure determination of **5·BCl₂** confirmed the incorporation of both Ga and B (Fig. 5). However, concomitant with exchange of Ga for B for the coordination to the heterocycle nitrogen atom, the latter has undergone an unprecedented change from a P,N to a C,N binding pocket.

The boron atom is incorporated in a rare four-membered ring that is fused to a rearomatized pyridine ring (judging from the almost identical carbon–carbon bond lengths in the ring). The carbon atom binds to boron while the pendant phosphine binds the trichlorogallane. The C1–B1 bond length of 1.682(3) Å likely reflects the ring-strain in this structure. To the best of our knowledge, this is the first example wherein the

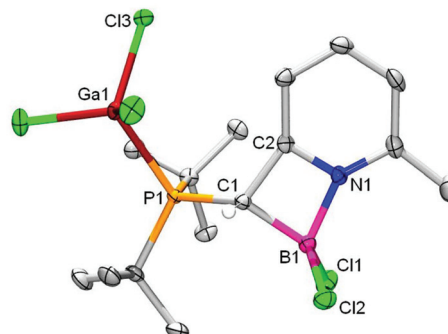
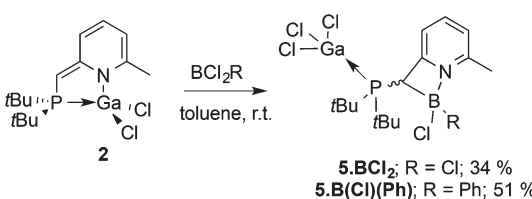


Fig. 5 Displacement ellipsoid plot (50% probability level) of **5·BCl₂**. Hydrogen atoms (apart from those on C1) are omitted for clarity. Selected bond lengths (Å) and angles (°): P1–C1 1.832(2); C1–C2 1.516(4); N1–C2 1.352(3); N1–B1 1.586(3); C1–B1 1.682(3); B1–Cl1 1.819(2); P1–Ga1 2.389(1); Ga1–Cl3 2.179(1); P1–C1–B1 132.2(2) (1); C2–C1–B1 84.4(2); C1–B1–N1 83.3(2); B1–N1–C2 93.9(2); N1–C2–C1 98.4(2); P1–C1–C2–N1–136.0.

methine spacer of a dearomatized lutidinylphosphine engages in direct coordination to a metal(loid). The only two structurally characterized fused heterobicyclic structures with boron and pyridine resulted either from (i) C–H activation of a lutidine-borenium adduct in the presence of an external Lewis base¹⁵ or (ii) ring-closure of a bis(pentafluorophenyl)boryl derived FLP.¹⁶ In both cases, extremely strong Lewis acids are involved.

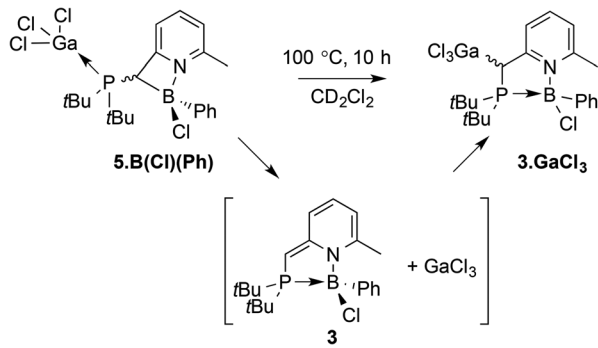
Given its unique nature, we decided to get further insight into the bonding situation within **5·BCl₂** by DFT calculations. Natural bond order (NBO) analysis demonstrated that the C1–B1 and the N1–B1 bonds are very polarized toward C and N (70% and 80%, respectively). In line with this observation, the Natural Population Analysis (NPA) showed a positively charged boron atom (+0.4). Interestingly, the C1 carbon atom bears a significant negative charge (–0.9). As a result, **5·BCl₂** is best described as the combination of a boronium and an anionic C,N ligand. The carbanion might be partially stabilized by negative hyperconjugation into the $\sigma^*(\text{P–C})$ orbitals as in reported α -monolithiated¹⁷ and α -dilithiated¹⁸ phosphine-boranes, although second order NBO analysis does not provide clear evidence for this. The analogous **5·B(Cl)(Ph)** was obtained as a mixture of diastereomers by reacting **2** with BCl_2Ph .

Compounds **3·GaCl₃** and **5·B(Cl)(Ph)** are linkage isomers (Scheme 6). The average DFT calculated energy differences of the linkage isomers **3·GaCl₃** and **5·B(Cl)(Ph)** (*syn* and *anti*) are within the upper limit of the precision of the methods (3.6 kcal mol^{–1} in favor of **5·B(Cl)(Ph)**). Given this small energy difference, we speculated that **5·B(Cl)(Ph)** could conceivably still be of relevance in the formal transmetallation of **2** with BCl_2Ph to provide **3·GaCl₃** under forcing conditions. To verify this hypothesis, a solution of **5·B(Cl)(Ph)** in CD_2Cl_2 was heated in a pressure tube to 100 °C for 6 hours, which cleanly generated **3·GaCl₃** as a mixture of diastereoisomers. It is plausible that this structural rearrangement, involving both C–B and



Scheme 5 Preparation of **5·BCl₂** and **5·B(Cl)(Ph)** by reaction of **2** with halaboranes.





Scheme 6 Thermal linkage isomerization of **5**·B(Cl)(Ph) into **3**·GaCl₃, proposedly with intermediacy of **3** and free GaCl₃.

P–Ga bond cleavage and C–Ga as well as P–B bond formation, proceeds *via* reconstitution of a mixture of **3** (with the dearomatized N-heterocycle) and GaCl₃, which were found to react instantaneously at room temperature.

With the well-defined coordination chemistry for the heterodinuclear species in hand, we wondered if the reaction of **1** with boron trichloride would also lead to selective trans-metallation and generation of product BCl₂(L) (as observed with GaCl₃) or an analogous reaction as observed for **3** to **5** but with a phosphino-alane pendant arm. The addition of one equivalent of BCl₃ to a solution of alane **1** at room temperature led to only 50% conversion of starting material, but the reaction smoothly went to completion when two equivalents of BCl₃ were used (Scheme 7).

The new species gives rise to a quadruplet in ³¹P NMR at δ 22.8, which is characteristic of the direct coordination of the phosphine to a boron atom. In line with the required stoichiometry, the ¹¹B NMR shows two signals, a doublet at δ 4.7 with a $^1J_{BP} = 139.4$ Hz and a broad singlet at δ 6.6. Single crystal X-ray structure determination of **6** confirmed the incorporation of two boron atoms in the molecule (Fig. 6). Complex **6** is structurally related to borane–gallane **5**·BCl₂, with the same strained four-membered ring including the boron atom, but featuring a trichloroborane-coordinated phosphine arm. It is likely that the interaction of AlClEt₂ with the pendant phosphine is relatively weak (perhaps partly due to steric hindrance), resulting in facile displacement by an additional equivalent of BCl₃.

In summary, we demonstrate the first examples of Group 13 complexes (boron, gallium and aluminum) stabilized by a dearomatized P,N ligand. Depending on the nature of the metal(loid) involved, very different reactivity toward Group

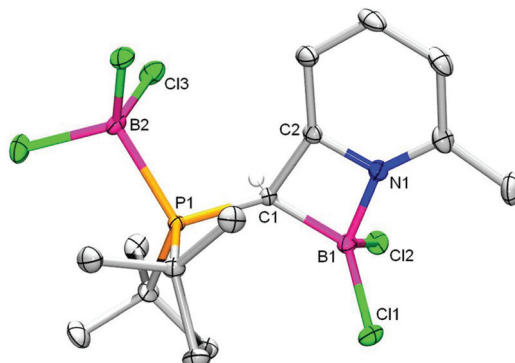


Fig. 6 Displacement ellipsoid plot (50% probability level) of **6**. Hydrogen atoms (apart from those on C1) are omitted for clarity. Selected bond lengths (Å) and angles (°): N1–B1 1.5805(25); B1–C1 1.6841(26); P1–B2 2.0441(21); C1–C2 1.5188(25); B1–Cl1 1.8220(21); B1–Cl2 1.8481(22); P1–C1 1.8419(19); N1–B1–C1 83.64(12); P1–C1–B1 133.05(13); N1–B1–Cl1 113.40(13); C1–P1–B2 105.87(8); P1–C1–C2–N1–135.23.

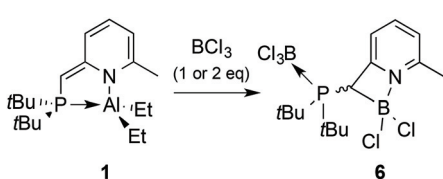
13 halogenides is observed. The rich coordination chemistry of this reactive ligand scaffold with G13 elements may open up *e.g.* new avenues for non-transition metal based small molecule activation and cooperative catalysis. Research in this direction is currently ongoing in our laboratories.

Experimental section

General comments

All reactions and manipulations were carried out under an atmosphere of dry dinitrogen using standard Schlenk techniques or in a glove-box. All solvents were purged with dinitrogen and dried using an MBRAUN Solvent Purification System (SPS). ¹H, ¹³C, ³¹P, ¹¹B and ²⁷Al NMR spectra were recorded on Bruker AV 300, Bruker DRX 300 or Bruker AV 400 spectrometers. Chemical shifts were expressed in positive sign, in parts per million, calibrated to residual ¹H (5.32 ppm) and ¹³C (53.84 ppm) solvent signals, external BF₃·Et₂O, 85% H₃PO₄ and Al(NO₃)₃ 1 M in D₂O (0 ppm) respectively. Mass spectra were recorded on an AccuTOF LC, JMS-T100LP or an AccuTOF GC v 4 g, JMS-T100GCV Mass spectrometer. Di-(*tert*-butylphosphino)methyl-6-methyl-pyridine **L^H** was prepared according to a literature procedure.¹⁹

Complex 1. A solution of *n*BuLi (2.5 M in hexanes, 0.25 mL, 0.63 mmol, 1 eq.) was added dropwise to an ice-cooled stirred solution of 2-(*di-tert*-butylphosphino)methyl-6-methyl-pyridine **L^H** (157 mg, 0.63 mmol) in diethylether (6.5 mL) and the resulting orange solution was allowed to react for 1 h at the same temperature. Then, the reaction mixture was cooled down to -78 °C and chlorodiethylaluminum (0.32 M in toluene, 1.98 mL, 1.01 eq.) was added dropwise. The reaction mixture was allowed to warm up to room temperature over 1 h, giving an orange solution and a white precipitate. After elimination of the salts by filtration and removal of the volatiles under reduced pressure, **1** was obtained as a red oil in 95% yield.



Scheme 7 Synthesis of **6** by transmetallation of **1** with 2 equiv. BCl₃.

¹H NMR (300 MHz, CD₂Cl₂, δ): 0.18 (m, 4H, CH₂Et), 1.05 (t, 6H, $^3J_{HH}$ = 8.0 Hz, CH₃Et), 1.25 (d, 18H, $^3J_{HP}$ = 13.9 Hz, tBu), 2.06 (s, 3H, CH₃Me), 3.46 (s br., 1H, C=C(H)(PtBu₂)), 5.28 (d, 1H, $^3J_{HH}$ = 6.5 Hz, C_{sp²}-H), 6.07 (d, 1H, $^3J_{HH}$ = 9.1 Hz, C_{sp²}-H), 6.42 (ddd, 1H, $^3J_{HH}$ = 9.1 Hz, $^3J_{HH}$ = 6.5 Hz, $^5J_{HP}$ = 1.5 Hz, C_{sp²}-H). ³¹P {¹H} NMR (121 MHz, CD₂Cl₂, δ): -0.9 (br.). ²⁷Al {¹H} NMR (78 MHz, CD₂Cl₂, δ): 162 (br.) ¹³C {¹H} NMR (75 MHz, CD₂Cl₂, δ): 2.5 (br., 2C, CH₂Et), 9.5 (s, 2C, CH₃Et), 23.1 (s, 1C, CH₃), 29.3 (d, 6C, $^2J_{CP}$ = 4.8 Hz, CH₃tBu), 34.3 (d, 2C, $^1J_{CP}$ = 23.5 Hz, P-C_{tBu}), 57.4 (d, 1C, $^1J_{CP}$ = 50.5 Hz, P-C_{sp²}), 102.7 (s, 1C, C_{sp²}-H), 118.1 (d, 1C, J_{CP} = 12.4 Hz, C_{sp²}-H), 133.9 (d, 1C, J_{CP} = 2.5 Hz, C_{sp²}-H), 150.9 (d, 1C, J_{CP} = 4.4 Hz, C_{quat.}), 167.2 (d, 1C, J_{CP} = 14.9 Hz, C_{quat.}). The highly air-sensitive nature of this oil (slow decomposition even in an N₂-filled glovebox) interfered during our repetitive attempts to obtain high-resolution mass analysis and elemental analysis.

Complex 2. Gallium trichloride (350.3 mg, 1.99 mmol, 1 eq.) in toluene (5 mL) was added dropwise to an *in situ* prepared solution of **1** (667.3 mg, 1.99 mmol) in diethyl ether (25 mL) under stirring at room temperature and the resulting mixture was stirred for an additional 4.5 h. Then, volatiles were removed under vacuum leading to an orange residue. This residue was extracted with a mixture of dichloromethane/pentane (0.3 mL/10 mL) and filtered. The resulting solution was concentrated to 2 mL, resulting in the crystallization of **2** at room temperature as sticky orange blocks in 96% yield. Crystals suitable for X-ray crystallography were obtained from a saturated solution of **2** in a toluene/diethylether mixture at room temperature. ¹H NMR (300 MHz, CD₂Cl₂, δ): 1.40 (d, 18H, $^3J_{HP}$ = 16.1 Hz, tBu), 2.35 (s, 3H, CH₃), 3.46 (d, 1H, $^2J_{HP}$ = 3.3 Hz, C=C(H)(PtBu₂)), 5.53 (d, 1H, J_{HH} = 6.6 Hz, C_{sp²}-H), 6.24 (d, 1H, J_{HH} = 9.0 Hz, C_{sp²}-H), 6.62 (ddd, 1H, J_{HH} = 9.0 Hz, J_{HH} = 6.6 Hz, J_{HP} = 1.3 Hz, C_{sp²}-H). ³¹P {¹H} NMR (121 MHz, CD₂Cl₂, δ): -3.1 (br.). ¹³C {¹H} NMR (75 MHz, CD₂Cl₂, δ): 22.7 (s, 1C, CH₃), 28.9 (d, 6C, $^2J_{CP}$ = 2.8 Hz, CH₃tBu), 36.8 (d, 2C, $^1J_{CP}$ = 30.4 Hz, P-C_{tBu}), 50.7 (d, 1C, $^1J_{CP}$ = 67.6 Hz, P-C_{sp²}), 105.5 (d, 1C, J_{CP} = 1.2 Hz, C_{sp²}-H), 119.2 (d, 1C, J_{CP} = 12.0 Hz, C_{sp²}-H), 135.7 (d, 1C, J_{CP} = 2.3 Hz, C_{sp²}-H), 151.2 (d, 1C, J_{CP} = 4.3 Hz, C_{quat.}), 166.7 (d, 1C, J_{CP} = 6.7 Hz, C_{quat.}). HRMS (FD): exact mass (monoisotopic) calcd for [C₁₅H₂₅⁶⁹GaNP³⁵Cl₂ + H]⁺, 390.04357; found 390.04338. Despite several attempts, no satisfactory combustion analysis data was obtained for this compound, likely as a result of its air-sensitive nature.

Complex 3. A solution of *n*BuLi (2.5 M in hexanes, 0.21 mL, 0.52 mmol, 1 eq.) was added dropwise under stirring to an ice-cooled solution of 2-(di-*tert*-butylphosphino)methyl-6-methylpyridine (150 mg, 0.52 mmol) in diethylether (5 mL) and the resulting orange solution was allowed to react for 1 h at the same temperature. Then, the reaction mixture was cooled down to -78 °C and dichlorophenylborane (77 μ L, 0.52 mmol, 1 eq.) was added dropwise. The reaction mixture was allowed to warm up to room temperature over 30 minutes and was further stirred for 1 h at room temperature, giving an orange solution and a white precipitate. Only **3** was detected in the crude mixture by ³¹P {¹H} NMR analysis. After removal of the volatiles, the residue was extracted with pentane (3 mL) and

dried affording the expected compound in a mixture with the starting material (7.7/1) (yield = 53%) due to partial hydrolysis. ¹H NMR (300 MHz, CD₂Cl₂, δ): 0.95 (d, 9H, $^3J_{HP}$ = 13.7 Hz, tBu), 1.51 (d, 9H, $^3J_{HP}$ = 13.3 Hz, tBu), 1.92 (s, 3H, CH₃), 3.46 (d, 1H, $^2J_{HP}$ = 5.1 Hz, C=C(H)(PtBu₂)), 5.40 (d, 1H, $^3J_{HH}$ = 6.5 Hz, C_{sp²}-H), 6.25 (d, 1H, J_{HH} = 8.9 Hz, C_{sp²}-H), 6.59 (ddd, 1H, J_{HH} = 8.9 Hz, J_{HH} = 6.5 Hz, $^5J_{HP}$ = 1.4 Hz, C_{sp²}-H), 7.10-7.24 (m, 3H, C_{sp²}-H), 7.33 (t, 1H, $^3J_{HH}$ = 7.4 Hz, C_{sp²}-H), 7.91 (d, 1H, J_{HH} = 7.4 Hz, C_{sp²}-H). ¹¹B {¹H} NMR (96 MHz, CD₂Cl₂, δ): 5.1 (d, $^1J_{BP}$ = 106.0 Hz). ³¹P {¹H} NMR (121 MHz, CD₂Cl₂, δ): 24.5 (s br.). ¹³C {¹H} NMR (75 MHz, CD₂Cl₂, δ): 22.6 (s, 1C, CH₃), 28.7 (s, 3C, CH₃tBu), 29.4 (s, 3C, CH₃tBu), 34.7 (d, 1C, $^1J_{CP}$ = 24.4 Hz, P-C_{tBu}), 38.8 (d, 1C, $^1J_{CP}$ = 23.1 Hz, P-C_{tBu}), 53.0 (d, 1C, $^1J_{CP}$ = 65.2 Hz, P-C_{sp²}), 106.0 (d, 1C, J_{CP} = 1.7 Hz, C_{sp²}-H), 116.2 (d, 1C, J_{CP} = 14.3 Hz, C_{sp²}-H), 127.2 (d, 1C, J_{CP} = 1.2 Hz, C_{sp²}-H), 127.3 (d, 1C, J_{CP} = 2.3 Hz, C_{sp²}-H), 127.8 (d, 1C, J_{CP} = 1.6 Hz, C_{sp²}-H), 133.4 (d, 1C, J_{CP} = 2.9 Hz, C_{sp²}-H), 135.0 (d, 1C, J_{CP} = 2.1 Hz, C_{sp²}-H), 136.0 (d, 1C, J_{CP} = 2.3 Hz, C_{sp²}-H), 151.3 (d, 1C, J_{CP} = 9.1 Hz, C_{quat.}), 167.6 (d, 1C, J_{CP} = 13.8 Hz, C_{quat.}), the aromatic carbon connected to boron is not observed. HRMS (CSI, -30 °C): exact mass (monoisotopic) calcd for [C₂₁H₃₀BClNP + H]⁺, 374.1976; found 374.1980. This compound proved too hydrolysis-sensitive for satisfactory combustion analysis data.

Complex anti-3-GaCl₃. A solution of **3** (445 mg, 1.19 mmol) in ether (15 mL) was added slowly to a solution of gallium trichloride (210 mg, 1.19 mmol, 1 eq.) in toluene (4 mL) at r. t. under stirring. The reaction mixture was then further stirred for 30 minutes leading to an orange solution and a yellowish precipitate. After removal of the mother liquor *via* cannula filtration, the precipitate was extracted with dichloromethane (20 mL), filtered and the limpid dichloromethane solution thus obtained was layered with pentane (21 mL), affording colorless crystals of *anti*-3-GaCl₃ in a yield of 40%. Crystals suitable for X-ray diffraction analysis were obtained under the same conditions. ¹H NMR (300 MHz, CD₂Cl₂, δ): 1.31 (d, 9H, $^3J_{HP}$ = 15.8 Hz, tBu), 1.50 (d, 9H, $^3J_{HP}$ = 13.6 Hz, tBu), 2.42 (s, 3H, CH₃), 3.67 (d, 1H, $^2J_{HP}$ = 13.4 Hz, P-C(H)-Ga), 7.04 (m, 1H, H_{arom.}), 7.18 (m, 1H, H_{arom.}), 7.29 (m, 1H, H_{arom.}), 7.34 (m, 1H, H_{arom.}), 7.43 (m, 1H, H_{arom.}), 7.96-8.05 (m, 2H, H_{arom.}), 8.51 (d, 1H, J_{HH} = 8.2 Hz, H_{arom.}). ³¹P {¹H} NMR (121 MHz, CD₂Cl₂, δ): 34.0 (br.). ¹¹B {¹H} NMR (96 MHz, CD₂Cl₂, δ): 5.6. ¹³C {¹H} NMR (75 MHz, CD₂Cl₂, δ): 23.4 (s, 1C, CH₃), 28.8 (s, 3C, CH₃tBu), 30.0 (s, 3C, CH₃tBu), 32.6 (br., P-C(H)-Ga), 36.6 (d, 1C, $^1J_{CP}$ = 24.4 Hz, P-C_{tBu}), 39.6 (d, 1C, $^1J_{CP}$ = 23.1 Hz, P-C_{tBu}), 123.5 (d, 1C, J_{CP} = 9.2 Hz, CH_{arom.}), 127.1 (d, 1C, J_{CP} = 1.9 Hz, CH_{arom.}), 128.4 (s, 2C, CH_{arom.}), 129.2 (d, 1C, J_{CP} = 2.3 Hz, CH_{arom.}), 134.7 (d, 1C, J_{CP} = 2.2 Hz, CH_{arom.}), 135.1 (d, 1C, J_{CP} = 2.9 Hz, CH_{arom.}), 143.0 (d, 1C, J_{CP} = 1.7 Hz, CH_{arom.}), 157.9 (d, 1C, J_{CP} = 7.4 Hz, C_{quat.}), 164.5 (d, 1C, J_{CP} = 3.7 Hz, C_{quat.}), the aromatic carbon connected to boron is not observed. Anal. Calcd For C₂₁H₃₀BCl₄GaNP; C, 45.88; H, 5.50; N, 2.55. Found: C, 45.81; H, 5.43; N, 2.49. M. p.: decomposition above 200 °C.

Isomerization of anti-3-GaCl₃. A solution of *anti*-3-GaCl₃ (14.6 mg, 26.6 μ mol) in CD₂Cl₂ (0.4 mL) was heated at 100 °C



for 10 h, leading to partial isomerization to its diastereoisomer *syn*-3·GaCl₃ in a 0.70/1.0 (*anti/syn*) ratio (as determined by integration of each =CHPPh₂ signal in the ¹H NMR spectrum, *D*1 = 10 s). The mixture of diastereoisomers was fully characterized by NMR spectroscopy: *anti*-3·GaCl₃ = A; *syn*-3·GaCl₃ = B. ¹H NMR (400 MHz, CD₂Cl₂, δ): 1.29 (d, 9H, $^3J_{\text{HP}} = 15.2$ Hz, *t*Bu(B)), 1.31 (d, 9H, $^3J_{\text{HP}} = 15.5$ Hz, *t*Bu(A)), 1.50 (d, 9H, $^3J_{\text{HP}} = 13.3$ Hz, *t*Bu(A)), 1.53 (d, 9H, $^3J_{\text{HP}} = 12.7$ Hz, *t*Bu(B)), 2.42 (s, 3H, CH₃(A)), 2.53 (s, 3H, CH₃(B)), 3.27 (d, 1H, $^2J_{\text{HP}} = 13.6$ Hz, P-C(H)-Ga (B)), 3.68 (d, 1H, $^2J_{\text{HP}} = 13.5$ Hz, P-C(H)-Ga (A)), 6.44 (d, 1H, $^3J_{\text{HH}} = 7.7$ Hz, H_{arom.}(B)), 7.04 (m, 1H, H_{arom.}(A)), 7.14–7.21 (m, 1H_{arom.}(A) + 1H_{arom.}(B)), 7.26–7.37 (m, 2H_{arom.}(A) + 1H_{arom.}(B)), 7.95–8.04 (m, 1H_{arom.}(A) + 1H_{arom.}(B)), 8.07 (d br., 1H, $^3J_{\text{HH}} = 7.4$ Hz, H_{arom.}(B)), 8.13 (t, 1H, $^3J_{\text{HH}} = 8.0$ Hz, H_{arom.}(B)), 8.51 (d, 1H, $^3J_{\text{HH}} = 8.5$ Hz, H_{arom.}(A)), 8.60 (d, 1H, $^3J_{\text{HH}} = 8.1$ Hz, H_{arom.}(B)). ³¹P {¹H} NMR (162 MHz, CD₂Cl₂, δ): 34.1 (br., A), 43.4 (br., B). ¹¹B {¹H} NMR (128 MHz, CD₂Cl₂, δ): 5.3 (br.). ¹³C {¹H} NMR (101 MHz, CD₂Cl₂, δ): 23.4 (s, 1C, CH₃(A)), 24.4 (s, 1C, CH₃(B)), 28.1 (br., 1C, P-C(H)-Ga(B)), 28.8 (s, 1C, CH₃*t*Bu(A)), 29.3 (s, 2C, CH₃*t*Bu(B)), 30.0 (s, 1C, CH₃*t*Bu(A)), 32.6 (br., 1C, P-C(H)-Ga(A)), 35.2 (d, 1C, $^1J_{\text{CP}} = 23.7$ Hz, P-C(*t*Bu)(B)), 36.6 (d, 1C, $^1J_{\text{CP}} = 24.5$ Hz, P-C(*t*Bu)(A)), 38.3 (d, 1C, $^1J_{\text{CP}} = 22.2$ Hz, P-C(*t*Bu)(B)), 39.5 (d, 1C, $^1J_{\text{CP}} = 23.0$ Hz, P-C(*t*Bu)(A)), 123.5 (d, 1C, $J_{\text{CP}} = 9.1$ Hz, CH_{arom.}(A)), 126.2 (d, 1C, $J_{\text{CP}} = 7.8$ Hz, CH_{arom.}(B)), 127.1 (d, 1C, $J_{\text{CP}} = 1.9$ Hz, CH_{arom.}(A)), 128.4 (br., 2C, CH_{arom.}(A)), 128.7 (br., 1C, CH_{arom.}(B)), 128.9 (d, 1C, $J_{\text{CP}} = 2.4$ Hz, CH_{arom.}(B)), 129.0 (br., 1C, CH_{arom.}(B)), 129.2 (d, 1C, $J_{\text{CP}} = 2.4$ Hz, CH_{arom.}(A)), 129.4 (d, 1C, $J_{\text{CP}} = 2.2$ Hz, CH_{arom.}(B)), 131.6 (s br., 1C, CH_{arom.}(B)), 134.7 (d, 1C, $J_{\text{CP}} = 2.2$ Hz, CH_{arom.}(A)), 135.1 (d, 1C, $J_{\text{CP}} = 2.9$ Hz, CH_{arom.}(A)), 136.1 (s br., 1C, CH_{arom.}(B)), 143.0 (d, 1C, $J_{\text{CP}} = 1.6$ Hz, CH_{arom.}(A)), 143.9 (s br., 1C, CH_{arom.}(B)), 157.9 (d, 1C, $J_{\text{CP}} = 7.8$ Hz, C_{quat.}(A)), 159.0 (d, 1C, $J_{\text{CP}} = 7.2$ Hz, C_{quat.}(B)), 161.3 (d, 1C, $J_{\text{CP}} = 2.5$ Hz, C_{quat.}(B)), 164.4 (d, 1C, $J_{\text{CP}} = 3.7$ Hz, C_{quat.}(A)), the aromatic *ipso*-carbon connected to boron is not observed for A or B.

Complex 4. A solution of hydrochloric acid in diethylether (1 M, 86 μ L, 1.1 eq.) was added dropwise to a suspension of *anti*-3·GaCl₃ (42 mg, 78.4 μ mol) in dichloromethane (2 mL) at -78 °C and the resulting suspension was allowed to warm up to room temperature overnight to give a colorless solution. The solution was filtered *via* cannula, the reaction flask was washed with dichloromethane (1 mL) and the organic layers were combined. The dichloromethane solution was layered with pentane (8 mL), affording colorless crystals of **4** with a yield of 89% at room temperature after one day. Crystals suitable for X-ray diffraction analysis were obtained by layering a dichloromethane solution of **4** with pentane at room temperature. ¹H NMR (300 MHz, CD₂Cl₂, δ): 1.14 (d, 9H, $^3J_{\text{HP}} = 15.3$ Hz, *t*Bu), 1.49 (d, 9H, $^3J_{\text{HP}} = 14.3$ Hz, *t*Bu), 2.59 (s, 3H, CH₃), 3.85–4.08 (m, 2H, CH₂), 6.29 (d, 1H, $J_{\text{HH}} = 7.4$ Hz, H_{arom.}), 7.19 (t, 1H, $J_{\text{HH}} = 7.4$ Hz, H_{arom.}), 7.37 (t br., 1H, $J_{\text{HH}} = 7.5$ Hz, H_{arom.}), 7.52 (t, 1H, $J_{\text{HH}} = 7.5$ Hz, H_{arom.}), 7.61 (d, 1H, $J_{\text{HH}} = 7.8$ Hz, H_{arom.}), 8.05 (m, 2H, H_{arom.}), 8.30 (t, 1H, $J_{\text{HH}} = 7.8$ Hz, H_{arom.}). ³¹P {¹H} NMR (121 MHz, CD₂Cl₂, δ): 21.4 (br.). ¹¹B {¹H} NMR (96 MHz, CD₂Cl₂, δ): 5.9 (br.). ¹³C {¹H} NMR (75 MHz,

CD₂Cl₂, δ): 23.6 (s, 1C, CH₃), 23.7 (d, 1C, $^1J_{\text{CP}} = 27.8$ Hz, CH₂), 28.8 (s, 3C, CH₃*t*Bu), 29.1 (s, 3C, CH₃*t*Bu), 35.2 (d, 1C, $^1J_{\text{CP}} = 18.6$ Hz, P-C(*t*Bu)), 37.3 (d, 1C, $^1J_{\text{CP}} = 21.1$ Hz, P-C(*t*Bu)), 125.0 (d, 1C, $J_{\text{CP}} = 7.5$ Hz, CH_{arom.}), 129.0 (d, 1C, $J_{\text{CP}} = 2.3$ Hz, CH_{arom.}), 129.5 (d, 1C, $J_{\text{CP}} = 2.3$ Hz, CH_{arom.}), 130.0 (d, 1C, $J_{\text{CP}} = 3.0$ Hz, CH_{arom.}), 130.5 (d, 1C, $J_{\text{CP}} = 2.3$ Hz, CH_{arom.}), 131.5 (d, 1C, $J_{\text{CP}} = 2.3$ Hz, CH_{arom.}), 135.2 (d, 1C, $J_{\text{CP}} = 3.0$ Hz, CH_{arom.}), 145.3 (d, 1C, $J_{\text{CP}} = 0.8$ Hz, CH_{arom.}), 156.0 (d, 1C, $J_{\text{CP}} = 3.0$ Hz, C_{quat.}), 159.7 (d, 1C, $J_{\text{CP}} = 6.8$ Hz, C_{quat.}) the aromatic carbon connected to boron is not observed. Anal. Calcd For C₂₁H₃₁BCl₅GaNP; C, 43.03; H, 5.33; N, 2.39. Found: C, 42.87; H, 5.20; N, 2.38. M. p.: 205–209 °C.

Complex 5-BCl₂. Boron trichloride in toluene (1 M, 0.65 mL, 0.65 mmol, 1 eq.) was added dropwise at room temperature to a solution of **2** (255 mg, 0.65 mmol) in toluene (5 mL) under stirring. Upon addition, the solution changed from orange to colorless. Then, pentane (20 mL) was added and the reaction mixture was slowly concentrated until a white powder precipitated. After removal of the supernatant *via* cannula filtration, the solid material was dried under reduced pressure. The solid was then dissolved in dichloromethane (3 mL) and filtered again. Layering of this solution with pentane (8 mL) led to the crystallization of **5-BCl₂** at room temperature in 3 days as colorless crystals with a yield of 34%. Crystals suitable for X-ray diffraction analysis were obtained by slow diffusion of pentane into a saturated dichloromethane solution of **5-BCl₂** at room temperature. ¹H NMR (300 MHz, CD₂Cl₂, δ): 1.54 (d, 9H, $^3J_{\text{HP}} = 16.8$ Hz, *t*Bu), 1.68 (d, 9H, $^3J_{\text{HP}} = 15.5$ Hz, *t*Bu), 2.75 (s, 3H, CH₃), 3.82 (d br., 1H, $^2J_{\text{HP}} = 12.3$ Hz, P-C(H)-B), 7.46 (d, 1H, $^3J_{\text{HH}} = 8.0$ Hz, H_{m-py}), 8.12 (pseudo-t, 1H, $^3J_{\text{HH}} = 8.0$ Hz, H_{p-py}), 8.32 (d, 1H, $^3J_{\text{HH}} = 8.1$ Hz, H_{m-py}). ³¹P {¹H} NMR (121 MHz, CD₂Cl₂, δ): 31.1 (br.). ¹¹B {¹H} NMR (96 MHz, CD₂Cl₂, δ): 6.4. ¹³C {¹H} NMR (75 MHz, CD₂Cl₂, δ): 18.1 (s, 1C, CH₃), 29.3 (d, 3C, $^2J_{\text{CP}} = 1.5$ Hz, CH₃*t*Bu), 30.3 (s, 3C, $^2J_{\text{CP}} = 2.5$ Hz, CH₃*t*Bu), 32.9–36.1 (br., 1C, P-C(H)-B), 37.5 (d, 1C, $^1J_{\text{CP}} = 20.8$ Hz, P-C(*t*Bu)), 38.5 (d, 1C, $^1J_{\text{CP}} = 15.2$ Hz, P-C(*t*Bu)), 123.8 (s, 1C, CH_{py}), 126.1 (s, 1C, CH_{py}), 144.7 (s, 1C, $J_{\text{CP}} = 1.2$ Hz, CH_{py}), 153.6 (s, 1C, C_{quat.}), 159.0 (s br., 1C, C_{quat.}). HRMS (CSI, -35 °C): exact mass (monoisotopic) calcd for [C₁₅H₂₅BCl₂NP – (GaCl₃) + H]⁺, 332.1276; found 332.1301. Anal. Calcd For C₁₅H₂₅BCl₅GaNP; C, 35.46; H, 4.96; N, 2.76. Found: C, 35.56; H, 4.86; N, 2.67. M. p.: decomposition above 177 °C.

Complex 5-B(Cl)(Ph). Dichlorophenylborane (49.8 μ L, 0.38 mmol, 1 eq.) in toluene (0.4 mL) was added dropwise at room temperature to a solution of **2** (155 mg, 0.38 mmol) in toluene (3 mL) under stirring, leading to a colorless solution. Analysis of the crude mixture by ¹H NMR showed the formation of a mixture of diastereoisomers in a 1.9/1 ratio. After removal of the volatiles under reduced pressure, the residue was dissolved in dichloromethane (4 mL) and filtered in order to have a limpid solution. Layering of this solution with pentane (14 mL) afforded colorless crystals of **5-B(Cl)(Ph)** in one day at room temperature with a yield of 51%. The mixture of diastereoisomers was fully characterized by NMR spectroscopy and the relative configuration of each isomer was attributed based on 2D NOESY NMR spectroscopy (in the case



of *syn*-5·BClPh, correlations are found between the B-C(H)-PPh₂ proton and the protons of the phenyl ring due to their spatial proximity, no correlation is observed with the *anti* isomer). For NMR: A = *syn*-5·B(Cl)(Ph); B = *anti*-5·B(Cl)(Ph). ¹H NMR (400 MHz, CD₂Cl₂, δ): 0.95 (d, 9H, ³J_{HP} = 16.4 Hz, *t*Bu(B)), 1.44 (d, 9H, ³J_{HP} = 15.4 Hz, *t*Bu(A)), 1.61 (d, 9H, ³J_{HP} = 17.9 Hz, *t*Bu(A)), 1.61 (d, 9H, ³J_{HP} = 15.0 Hz, *t*Bu(B)), 2.30 (s, 3H, CH₃(A)), 2.48 (s, 3H, CH₃(B)), 3.74 (d, 1H, ²J_{HP} = 15.2 Hz, P-C(H)-B (B)), 3.77 (d, 1H, ²J_{HP} = 12.5 Hz, P-C(H)-B (A)), 7.23–7.42 (m, 5 H_{Ph} (B) and 5 H_{Ph} (A) and 1 H_{m-py} (A)), 7.49 (d, 1H, ³J_{HH} = 8.0 Hz, H_{m-py} (B)), 8.10 (pseudo-t, 1H, ³J_{HH} = 8.0 Hz, H_{p-py} (A)), 8.16 (pseudo-t, 1H, ³J_{HH} = 8.0 Hz, H_{p-py} (B)), 8.34 (d, 1H, ³J_{HH} = 8.1 Hz, H_{m-py} (B)), 8.38 (d, 1H, ³J_{HH} = 8.1 Hz, H_{m-py} (B)). ³¹P {¹H} NMR (121 MHz, CD₂Cl₂, δ): 32.6 (br.). ¹¹B {¹H} NMR (96 MHz, CD₂Cl₂, δ): 7.4. ¹³C {¹H} NMR (75 MHz, CD₂Cl₂, δ): 18.0 (s, 1C, CH₃(A)), 18.4 (s, 1C, CH₃(B)), 29.0 (s, 3C, CH_{3tBu}(B)), 29.2 (s, 3C, CH_{3tBu}(A)), 29.5 (s, 3C, CH_{3tBu}(B)), 30.3 (d, 3C, ²J_{CP} = 2.1 Hz, CH_{3tBu}(A)), 32.8 (br., C-B(A) + C-B(B)), 37.1 (d, 1C, ¹J_{CP} = 22.7 Hz, P-C_{tBu}(B)), 37.3 (d, 1C, ¹J_{CP} = 21.8 Hz, P-C_{tBu}(A)), 37.6 (d, 1C, ¹J_{CP} = 16.8 Hz, P-C_{tBu}(B)), 38.5 (d, 1C, ¹J_{CP} = 15.9 Hz, P-C_{tBu}(A)), 123.7 (s, 1C, CH_{arom}(B)), 123.9 (s, 1C, CH_{arom}(A)), 125.4 (s, 1C, CH_{arom}(B)), 125.6 (s, 1C, CH_{arom}(A)), 127.9–128.6 (m, 3CH_{arom}(A) + 4CH_{arom}(B)), 128.7 (s, 1C, CH_{arom}(B)), 131.7 (s, 2C, CH_{arom}(A)), 143.6 (s, 1C, CH_{arom}(A)), 143.9 (s, 1C, CH_{arom}(B)), 153.6 (s, 1C, C_{quat}(A)), 154.1 (s, 1C, C_{quat}(B)), 160.7 (s, 1C, C_{quat}(A)), 161.1 (br., 1C, C_{quat}(B)), the aromatic *ipso*-carbon connected to boron is not observed for A or B. HRMS (CSI, –35 °C): exact mass (monoisotopic) calcd for [C₂₁H₂₉B₁Cl₁N₁P₁ – (GaCl₃) + H]⁺, 374.1980; found 374.2062. Anal. Calcd For C₂₁H₃₀B₁Cl₁GaNP; C, 45.88; H, 5.50; N, 2.55. Found: C, 45.61; H, 5.46; N, 2.50.

Isomerization of 5·BCl₂ to *anti*-3·GaCl₃ and *syn*-3·GaCl₃. A colorless solution of 5·B(Cl)(Ph) (33.3 mg, 60.6 μ mol) in CD₂Cl₂ (0.4 ml) was heated to 100 °C in an NMR tube for 10 h, leading to a yellow solution. Monitoring of the reaction by ¹H NMR spectroscopy (internal standard = toluene 5 μ L) showed the formation of a mixture of diastereoisomers 3·GaCl₃ *anti*, 56%; *syn*, 38%) and traces of decomposition product 4 (3%). The latter probably results from the addition of HCl (as traces in the solvent) across the C–Ga bond of 3·GaCl₃.

Complex 6. To a solution of 1 (535.0 mg, 1.59 mmol) in diethylether (20 mL) was added BCl₃ (1 M in solution in toluene; 3.18 mL, 3.18 mmol, 2 eq.) at room temperature under stirring, resulting in a colorless solution. After removal of the volatiles under reduced pressure, the residue was dissolved in dichloromethane, filtered and layered with pentane to give the expected compound 6 as colorless crystals with a yield of 48%. Single crystals suitable for X-ray diffraction analysis were obtained using the same conditions. ¹H NMR (300 MHz, CD₂Cl₂, δ): 1.59 (d, 9H, ³J_{HP} = 14.9 Hz, *t*Bu), 1.68 (d, 9H, ³J_{HP} = 13.4 Hz, *t*Bu), 2.75 (s, 3H, CH₃), 3.93 (d, 1H, ²J_{HP} = 15.3 Hz, P-C(H)-B), 7.42 (d, 1H, ³J_{HH} = 8.0 Hz, H_{m-py}), 8.06 (pseudo-t, 1H, ³J_{HH} = 8.1 Hz, H_{p-py}), 8.48 (d, 1H, ³J_{HH} = 8.3 Hz, H_{m-py}). ³¹P {¹H} NMR (121 MHz, CD₂Cl₂, δ): 22.8 (q, ¹J_{PB} = 139.4 Hz). ¹¹B {¹H} NMR (96 MHz, CD₂Cl₂, δ): 4.7 (d, ¹J_{PB} = 139.4 Hz, P-BCl₃), 6.6 (br., BCl₂). ¹³C {¹H} NMR (75 MHz, CD₂Cl₂, δ): 18.0 (s, 1C,

CH₃), 29.4 (s, 3C, CH_{3tBu}), 30.0 (s, 3C, CH_{3tBu}), 35.2 (br., 1C, B-C), 37.4 (d, 1C, ¹J_{CP} = 27.0 Hz, P-C_{tBu}), 38.0 (d, 1C, ¹J_{CP} = 21.1 Hz, P-C_{tBu}), 124.9 (s, 1C, CH_{m-py}), 125.7 (s, 1C, CH_{m-py}), 144.3 (s, 1C, CH_{p-py}), 153.0 (s, 1C, C_{o-py}), 159.7 (s br., 1C, C_{o-py}). Anal. Calcd For C₁₅H₂₅B₂Cl₅NP; C, 40.10; H, 5.61; N, 3.12. Found: C, 40.13; H, 5.63; N, 3.13.

X-ray crystallography

X-ray intensities were measured on a Bruker D8 Quest Eco diffractometer equipped with a Triumph monochromator (λ = 0.71073 Å) and a CMOS Photon 50 detector at a temperature of 150(2) K. Intensity data were integrated with the Bruker APEX2 software.²⁰ Absorption correction and scaling was performed with SADABS.²¹ The structures were solved with the program SHELXL.²⁰ Least-squares refinement was performed with SHELXL-2013²² against F^2 of all reflections. Non-hydrogen atoms were refined with anisotropic displacement parameters. The H atoms were placed at calculated positions using the instructions AFIX 13, AFIX 43 or AFIX 137 with isotropic displacement parameters having values 1.2 or 1.5 times U_{eq} of the attached C atoms. CCDC 1455266–1455269 contain the supplementary crystallographic data for this paper.

Details for 2. C₂₀H₂₅Cl₂GaNP, F_w = 451.00, colorless, 0.327 \times 0.210 \times 0.152 mm, monoclinic, $P2_1/c$ (no: 14), a = 9.049(3), b = 9.165(3), c = 22.163(9) Å, β = 91.028(8)°, V = 1837.9(20) Å³, Z = 4, D_x = 1.643 g cm⁻³, μ = 1.893 mm⁻¹. 39 709 reflections were measured up to a resolution of $(\sin \theta/\lambda)_{max}$ = 0.65 Å⁻¹. 7005 reflections were unique (R_{int} = 0.0634), of which 5482 were observed [I > 2 $\sigma(I)$]. 188 Parameters were refined with 0 restraints. R_1/wR_2 [I > 2 $\sigma(I)$]: 0.0329/0.0687. R_1/wR_2 [all refl.]: 0.0517/0.0752. S = 1.008. Residual electron density between –0.760 and 0.667 e Å⁻³. CCDC 1455266.

Details for *anti*-3·GaCl₃. C₂₁H₃₀B₁Cl₁GaNP, F_w = 549.76, colorless, 0.478 \times 0.201 \times 0.199 mm, monoclinic, $P2_1/c$ (no: 14), a = 10.152(10), b = 16.382(9), c = 15.393(12) Å, β = 93.68(3)°, V = 2555.5(5) Å³, Z = 4, D_x = 1.467 g cm⁻³, μ = 1.609 mm⁻¹. 29 499 reflections were measured up to a resolution of $(\sin \theta/\lambda)_{max}$ = 0.84 Å⁻¹. 4370 reflections were unique (R_{int} = 0.0384), of which 3954 were observed [I > 2 $\sigma(I)$]. 269 Parameters were refined with 252 restraints. R_1/wR_2 [I > 2 $\sigma(I)$]: 0.0240/0.0563. R_1/wR_2 [all refl.]: 0.0288/0.0591. S = 1.091. Residual electron density between –0.382 and 0.431 e Å⁻³. CCDC 1455267.

Details for 4. C₂₁H₃₁B₁Cl₄GaNP, F_w = 550.77, colorless, 0.479 \times 0.452 \times 0.240 mm, triclinic, $P\bar{1}$ (no: 1), a = 9.7845(7), b = 11.8465(9), c = 12.0322(9) Å, α = 83.458(3), β = 83.640(3), γ = 77.501(3)°, V = 1347.41(17) Å³, Z = 2, D_x = 1.358 g cm⁻³, μ = 1.486 mm⁻¹. 70 054 reflections were measured up to a resolution of $(\sin \theta/\lambda)_{max}$ = 0.64 Å⁻¹. 10 873 reflections were unique (R_{int} = 0.0501), of which 8259 were observed [I > 2 $\sigma(I)$]. 278 Parameters were refined with 0 restraints. R_1/wR_2 [I > 2 $\sigma(I)$]: 0.377/0.746. R_1/wR_2 [all refl.]: 0.647/0.897. S = 1.076. Residual electron density between –1.04 and 0.86 e Å⁻³. CCDC 1455269.

Details for 5·BCl₂. C₁₅H₂₅B₂Cl₅GaNP, F_w = 508.11, colorless, 0.312 \times 0.268 \times 0.108 mm, triclinic, $P\bar{1}$ (no: 1), a = 8.483(6), b = 8.751(5), c = 16.791(7) Å, α = 87.39(2), β = 80.71(2), γ = 63.25(3)°, V = 1098.0(16) Å³, Z = 2, D_x = 1.560 g cm⁻³, μ = 1.963 mm⁻¹.



33 460 reflections were measured up to a resolution of $(\sin \theta/\lambda)_{\text{max}} = 0.74 \text{ \AA}^{-1}$. 5489 reflections were unique ($R_{\text{int}} = 0.0589$), of which 4453 were observed [$I > 2\sigma(I)$]. 224 Parameters were refined with 252 restraints. $R_1/\text{w}R_2$ [$I > 2\sigma(I)$]: 0.321/0.628. $R_1/\text{w}R_2$ [all refl.]: 0.491/0.685. $S = 1.008$. Residual electron density between -0.469 and 0.503 e \AA^{-3} . CCDC 1455268.

Details for 6. $\text{C}_{15}\text{H}_{25}\text{B}_2\text{Cl}_5\text{NP}$, $F_{\text{w}} = 449.20$, colorless, $0.391 \times 0.311 \times 0.184 \text{ mm}$, triclinic, $P\bar{1}$ (no: 1), $a = 8.2835(19)$, $b = 8.5491(18)$, $c = 16.876(4) \text{ \AA}$, $\alpha = 87.103(6)$, $\beta = 81.076(7)$, $\gamma = 61.850(5)^\circ$, $V = 1040.6(4) \text{ \AA}^3$, $Z = 2$, $D_x = 1.434 \text{ g cm}^{-3}$, $\mu = 0.773 \text{ mm}^{-1}$. 34 045 reflections were measured up to a resolution of $(\sin \theta/\lambda)_{\text{max}} = 0.75 \text{ \AA}^{-1}$. 5215 reflections were unique ($R_{\text{int}} = 0.658$), of which 4319 were observed [$I > 2\sigma(I)$]. 227 Parameters were refined with 0 restraints. $R_1/\text{w}R_2$ [$I > 2\sigma(I)$]: 0.357/0.722. $R_1/\text{w}R_2$ [all refl.]: 0.502/0.774. $S = 1.072$. Residual electron density between -0.32 and 0.58 e \AA^{-3} . CCDC 1481714.

DFT calculations

Calculations were carried out with the Gaussian09 software²³ at the DFT level, using the hybrid functional B3PW91.²⁴ Aluminum, gallium, chlorine and phosphorus atoms were treated with small-core pseudopotentials from the Stuttgart group, with additional polarization orbitals.²⁵ Nitrogen, carbon, boron and H atoms have been treated with the all-electron 6-31G** Pople basis set. The geometry optimizations were done without any symmetry constraints. Analytical calculations of the vibrational frequencies of the optimized geometries were performed to confirm that the structures obtained were minimums, and also obtained the thermal corrections over the energies. The Natural Bond Orbital analysis was done over the optimized structure, with the version of the NBO software included in Gaussian09.²⁶

Acknowledgements

This research is funded by the European Research Council through ERC Starting Grant *EuReCat* 279097 to J. I. v. d. V. We thank Prof.'s Bas de Bruin and Joost Reek for general support and interest in our work and Ed Zuidinga for MS analysis.

References

- 1 R. Kinjo, B. Donnadieu, M. A. Celik, G. Frenking and G. Bertrand, *Science*, 2011, **333**, 610; C. Fliedel, G. Schnee, T. Avilés and S. Dragoréne, *Coord. Chem. Rev.*, 2014, **275**, 63.
- 2 I. A. Cade and M. J. Ingleson, *Chem. – Eur. J.*, 2014, **20**, 12874; M. Devillard, R. Brousses, K. Miqueu, G. Bouhadir and D. Bourissou, *Angew. Chem., Int. Ed.*, 2015, **54**, 5722; J. M. Farrell, R. T. Posarathananathan and D. W. Stephan, *Chem. Sci.*, 2015, **6**, 2010; Z. Yang, M. Zhong, X. Ma, K. Nijesh, S. De, P. Parameswaran and H. W. Roesky, *J. Am. Chem. Soc.*, 2016, **138**, 2548.
- 3 D. W. Stephan, *J. Am. Chem. Soc.*, 2015, **137**, 10018; D. W. Stephan and G. Erker, *Angew. Chem., Int. Ed.*, 2015, **54**, 6400; D. W. Stephan, *Acc. Chem. Res.*, 2015, **48**, 306–316.
- 4 C. Gunanathan and D. Milstein, *Acc. Chem. Res.*, 2011, **44**, 588; K. Junge, K. Schröder and M. Beller, *Chem. Commun.*, 2011, **47**, 4849; J. I. van der Vlugt, *Eur. J. Inorg. Chem.*, 2012, 363; D. Gelman and S. Musa, *ACS Catal.*, 2012, **2**, 2456; W.-H. Wang, J. T. Muckerman, E. Fujita and Y. Himeda, *New J. Chem.*, 2013, **37**, 1860; S. Kuwata and T. Ikariya, *Chem. Commun.*, 2014, **50**, 14290; R. H. Morris, *Acc. Chem. Res.*, 2015, **48**, 1494.
- 5 Recent reviews: J. I. van der Vlugt and J. N. H. Reek, *Angew. Chem., Int. Ed.*, 2009, **48**, 8832; C. Gunanathan and D. Milstein, *Chem. Rev.*, 2014, **114**, 12024; J. R. Khusnutdinova and D. Milstein, *Angew. Chem., Int. Ed.*, 2015, **54**, 12236. See also: H. Li, B. Zheng and K.-W. Huang, *Coord. Chem. Rev.*, 2015, **293–294**, 116. Recent examples from our group: J. I. van der Vlugt, E. A. Pidko, D. Vogt, M. Lutz, A. L. Spek and A. Meetsma, *Inorg. Chem.*, 2008, **47**, 4442; J. I. van der Vlugt, M. Lutz, E. A. Pidko, D. Vogt and A. L. Spek, *Dalton Trans.*, 2009, 1016; S. Y. de Boer, Y. Gloaguen, J. N. H. Reek, M. Lutz and J. I. van der Vlugt, *Dalton Trans.*, 2012, **41**, 11276; S. Y. de Boer, Y. Gloaguen, M. Lutz and J. I. van der Vlugt, *Inorg. Chim. Acta*, 2012, **380**, 336; L. S. Jongbloed, B. de Bruin, J. N. H. Reek, M. Lutz and J. I. van der Vlugt, *Chem. – Eur. J.*, 2015, **21**, 7297; L. S. Jongbloed, B. de Bruin, J. N. H. Reek, M. Lutz and J. I. van der Vlugt, *Catal. Sci. Technol.*, 2016, **6**, 1320. See also: Y. Gloaguen, C. Rebreyend, M. Lutz, P. Kumar, M. I. Huber, J. I. van der Vlugt, S. Schneider and B. de Bruin, *Angew. Chem., Int. Ed.*, 2014, **53**, 6814; Z. Tang, S. Mandal, N. D. Paul, M. Lutz, P. Li, J. I. van der Vlugt and B. de Bruin, *Org. Chem. Front.*, 2015, **2**, 1561.
- 6 Two known alternative binding modes are via phosphorus only or with P and N both binding to a different metal center. For an example, see: J. I. van der Vlugt, E. A. Pidko, R. C. Bauer, Y. Gloaguen, M. K. Rong and M. Lutz, *Chem. – Eur. J.*, 2011, **17**, 3850.
- 7 Transmetallation of P-only coordinated mononuclear Ag-species to e.g. Pd has been reported: J. I. van der Vlugt, M. A. Siegler, M. Janssen, D. Vogt and A. L. Spek, *Organometallics*, 2009, **28**, 7025.
- 8 L. A. Körte, R. Warner, V. Y. Vishnevskiy, B. Neumann, H.-G. Stammmer and N. W. Mitzel, *Dalton Trans.*, 2015, **44**, 9992; J. Zheng, Y.-J. Lin and H. Wang, *Dalton Trans.*, 2016, **45**, 6088.
- 9 L.-C. Liang, M.-H. Huang and C.-H. Hung, *Inorg. Chem.*, 2004, **43**, 2166; H. Naka, M. Uchiyama, Y. Matsumoto, A. E. H. Wheatley, M. McPartlin, J. V. Morey and Y. Kondo, *J. Am. Chem. Soc.*, 2007, **129**, 1921.
- 10 J. I. van der Vlugt, E. A. Pidko, D. Vogt, M. Lutz and A. L. Spek, *Inorg. Chem.*, 2009, **48**, 7513; M. Montag, J. Zhang and D. Milstein, *J. Am. Chem. Soc.*, 2012, **134**, 10325; C. A. Huff, J. W. Kampf and M. S. Sanford, *Organometallics*, 2012, **31**, 4643; C. A. Huff, J. W. Kampf and

M. S. Sanford, *Chem. Commun.*, 2013, **49**, 7147; S. Perdriau, D. S. Zijlstra, H. J. Heeres, J. G. de Vries and E. Otten, *Angew. Chem., Int. Ed.*, 2015, **54**, 4236. See also: Z. Tang, E. Otten, J. N. H. Reek, J. I. van der Vlugt and B. de Bruin, *Chem. – Eur. J.*, 2015, **21**, 12683.

11 W. E. Piers, S. C. Bourke and K. D. Conroy, *Angew. Chem., Int. Ed.*, 2005, **44**, 5016.

12 J. L. Atwood and S. G. Bott, *J. Chem. Soc., Dalton Trans.*, 1987, 747; C.-W. Tsang, C. A. Rohrick, T. S. Saini, B. O. Patrick and D. P. Gates, *Organometallics*, 2002, **21**, 1008; C.-W. Tsang, C. A. Rohrick, T. S. Saini, B. O. Patrick and D. P. Gates, *Organometallics*, 2004, **23**, 5913; V. Bagutski, A. Del Grosso, J. A. Carillo, I. A. Cade, M. D. Helm, J. R. Lawson, P. J. Singleton, S. A. Solomon, T. Marcelli and M. J. Ingleson, *J. Am. Chem. Soc.*, 2013, **135**, 474.

13 A. Alzamly, S. Gambarotta and I. Korobkov, *Organometallics*, 2013, **32**, 7204; A. Anaby, B. Butschke, Y. Ben-David, L. J. W. Shimon, G. Leitus, M. Feller and D. Milstein, *Organometallics*, 2014, **33**, 3716; T. Cheisson and A. Auffrant, *Dalton Trans.*, 2016, **45**, 2069.

14 P. Kölle and H. Nöth, *Chem. Rev.*, 1985, **85**, 399; D. P. Gates, R. Ziembinski, I. Manners, A. L. Rheingold and B. S. Haggerty, *Angew. Chem., Int. Ed.*, 1994, **33**, 2277.

15 E. R. Clark, A. Del Grosso and M. J. Ingleson, *Chem. – Eur. J.*, 2013, **19**, 2462.

16 See ref. 8 and: J. Vergnaud, T. Ayed, K. Hussein, L. Vendier, M. Grellier, G. Bouhadir, J.-C. Barthelat, S. Sabo-Etienne and D. Bourissou, *Dalton Trans.*, 2007, 2370.

17 K. Izod, C. Wills, E. Anderson, R. W. Harrington and M. R. Probert, *Organometallics*, 2014, **33**, 5283.

18 H. Heuclin, S. Y.-F. Ho, X. F. Le Goff, C.-W. So and N. Mézailles, *J. Am. Chem. Soc.*, 2013, **135**, 8774.

19 E. Kinoshita, K. Arashiba, S. Kuriyama, Y. Miyake, R. Shimazaki, N. Haruyuki and N. Yoshiaki, *Organometallics*, 2012, **31**, 8437. See also our 2012 contributions in ref. 5.

20 Bruker, *APEX2 software*, Madison WI, USA, 2014.

21 G. M. Sheldrick, *SADABS*, Universität Göttingen, Germany, 2008.

22 G. M. Sheldrick, *SHELXL2013*, University of Göttingen, Germany, 2013.

23 M. J. Frisch, G. W. Trucks, H. B. Schlegel, G. E. Scuseria, M. A. Robb, J. R. Cheeseman, G. Scalmani, V. Barone, B. Mennucci, G. A. Petersson, H. Nakatsuji, M. Caricato, X. Li, H. P. Hratchian, A. F. Izmaylov, J. Bloino, G. Zheng, J. L. Sonnenberg, M. Hada, M. Ehara, K. Toyota, R. Fukuda, J. Hasegawa, M. Ishida, T. Nakajima, Y. Honda, O. Kitao, H. Nakai, T. Vreven, J. A. Montgomery Jr., J. E. Peralta, F. Ogliaro, M. Bearpark, J. J. Heyd, E. Brothers, K. N. Kudin, V. N. Staroverov, R. Kobayashi, J. Normand, K. Raghavachari, A. Rendell, J. C. Burant, S. S. Iyengar, J. Tomasi, M. Cossi, N. Rega, J. M. Millam, M. Klene, J. E. Knox, J. B. Cross, V. Bakken, C. Adamo, J. Jaramillo, R. Gomperts, R. E. Stratmann, O. Yazyev, A. J. Austin, R. Cammi, C. Pomelli, J. W. Ochterski, R. L. Martin, K. Morokuma, V. G. Zakrzewski, G. A. Voth, P. Salvador, J. J. Dannenberg, S. Dapprich, A. D. Daniels, Ö. Farkas, J. B. Foresman, J. V. Ortiz, J. Cioslowski and D. J. Fox, *Gaussian 09, Revision A.02*, Gaussian, Inc., Wallingford, CT, 2009.

24 A. D. Becke, *J. Chem. Phys.*, 1993, **98**, 5648; J. P. Perdew and Y. Wang, *Phys. Rev. B: Condens. Matter*, 1992, **45**, 13244; K. Burke, J. P. Perdew and W. Yang, *Electronic Density Functional Theory: Recent Progress and New Directions*, ed. J. F. Dobson, G. Vignale and M. P. Das, Plenum, New York, 1998.

25 A. Bergner, M. Dolg, W. Kuechle, H. Stoll and H. Preuss, *Mol. Phys.*, 1993, **80**, 1431; T. Leininger, A. Berning, A. Nicklass, H. Stoll, H.-J. Werner and H.-J. Flad, *Chem. Phys.*, 1997, **217**, 19.

26 E. D. Glendening, A. E. Reed, J. E. Carpenter and F. Weinhold, *NBO Version 3.1*.

